Flow and isotopic ratios from KRATTA@ASYEOS experiment

Jerzy Łukasik, Piotr Pawłowski, Paweł Lasko
IFJ PAN Kraków, Poland
Janusz Brzychczyk, Sebastian Kupny
Jagiellonian University, Kraków, Poland
and the ASY-EOS Collaboration

- ASY-EOS Experiment
- KRATTA results
- LAND results **(P. Russotto et al.)**

NUSYM16, Beijing, 13-17.06.2016

Work supported by Polish National Science Center (NCN),
Contract Nos. UMO-2013/10/M/ST2/00624, UMO-2013/09/B/ST2/04064

NATIONAL SCIENCE CENTRE
POLAND

ASY-EOS experimental setup

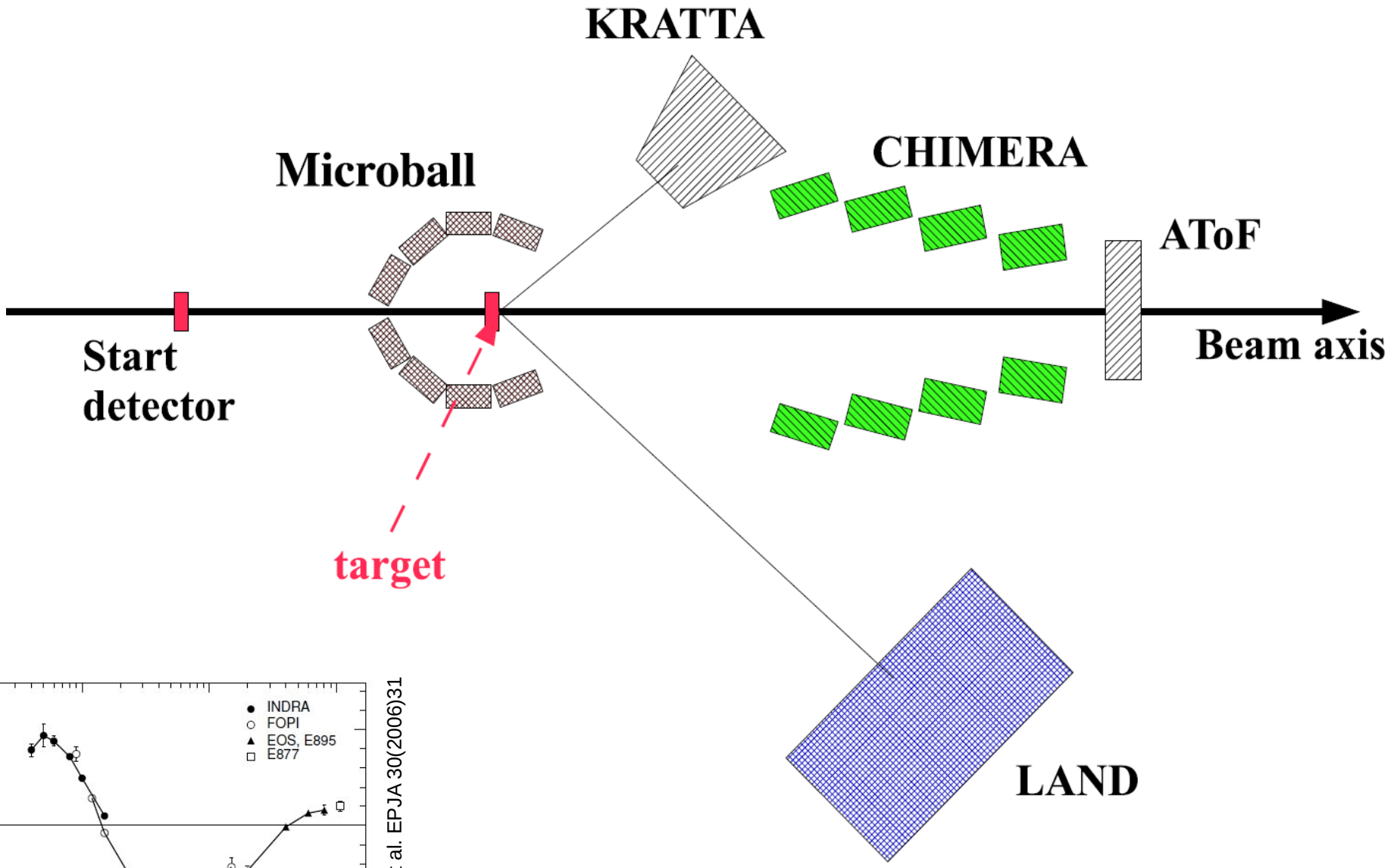

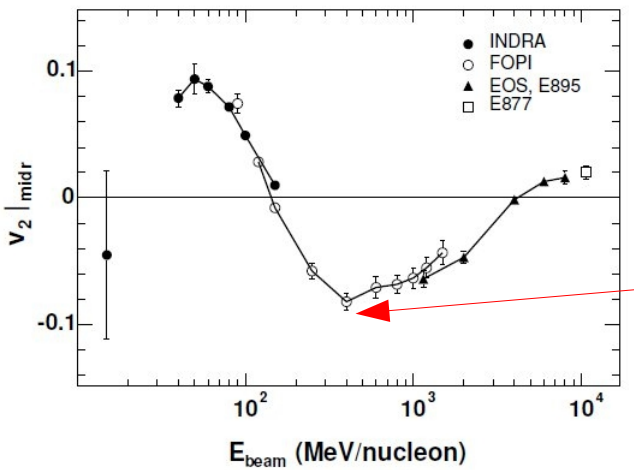

A. Andronic et al. EPJA 30(2006)31

^{197}Au	+	^{197}Au	@ 400 AMeV	$\delta^2 = 0.039$
^{96}Zr	+	^{96}Zr	@ 400 AMeV	$\delta^2 = 0.028$
^{96}Ru	+	^{96}Ru	@ 400 AMeV	$\delta^2 = 0.007$

ASY-EOS e[illegible]tal setup

KRATTA

5x7 triple telescopes, 20°<θ<60°
Si-CsI-CsI
Midrapidity pdt +
Isotopes of Z<7

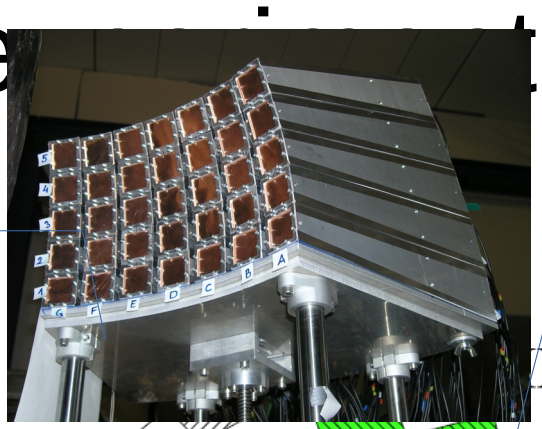

CHIMERA

4 rings, 352 CsI(Tl), 7°<θ<20°
Centrality
&
Reaction plane

Start + ROLU

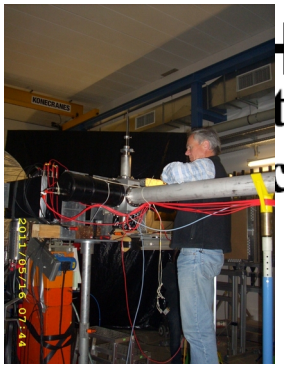

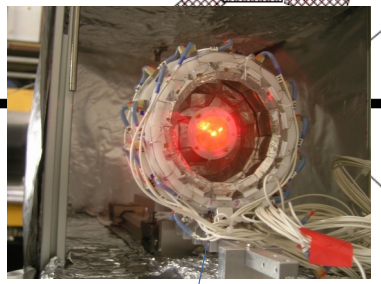

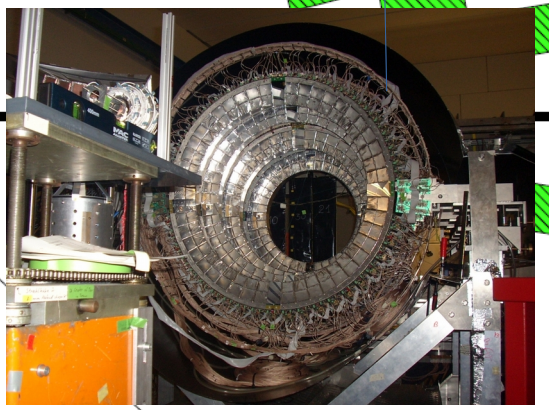

target

μ-Ball + Halo

4 rings, θ>60°, CsI(Tl)
Discriminate target vs air interactions, remove halo, possibly centrality + rpl

SHADOW BAR

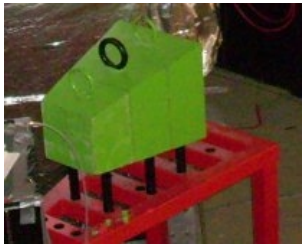

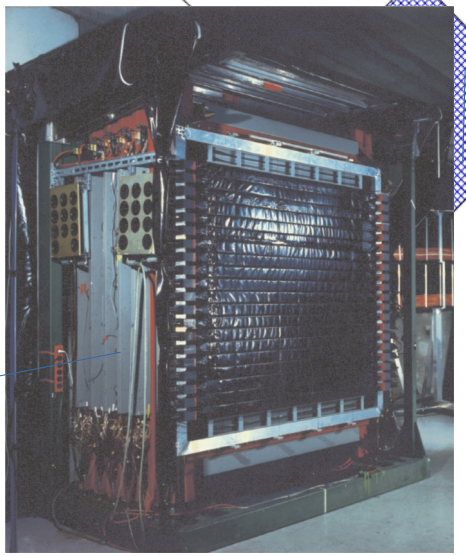

ALADIN ToF-Wall

96 plastic bars
x-y positions, centrality, reaction plane, trigger

LAND+VETO

2x2x1 m^3 plastic/Fe sandwich
+ plastic veto wall
Midrapidity neutrons & Z=1

ASY-EOS experimental setup

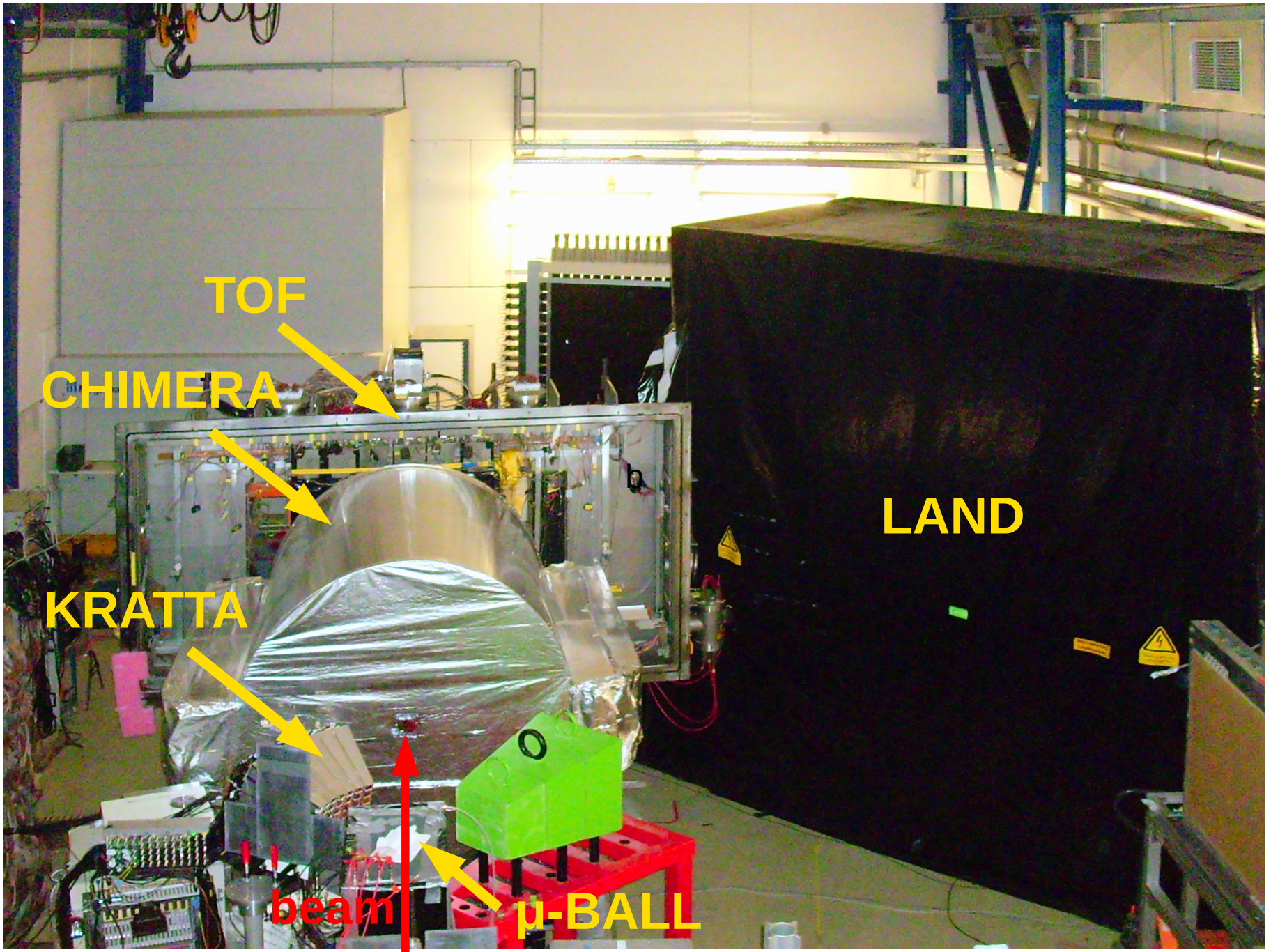

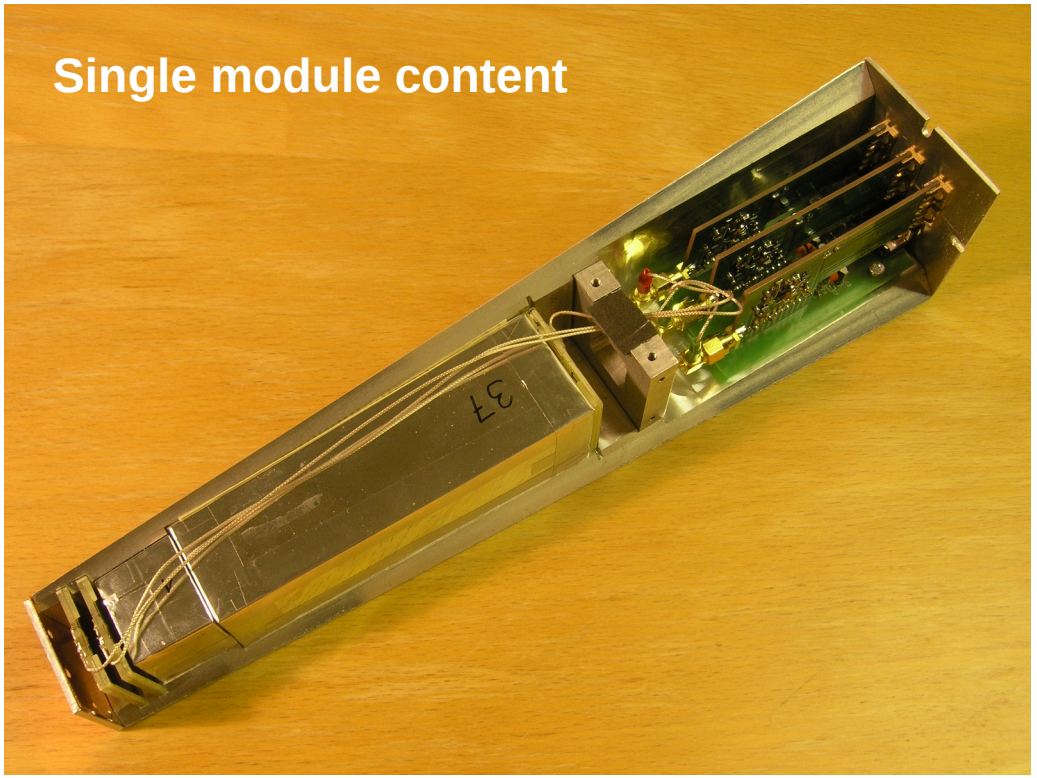

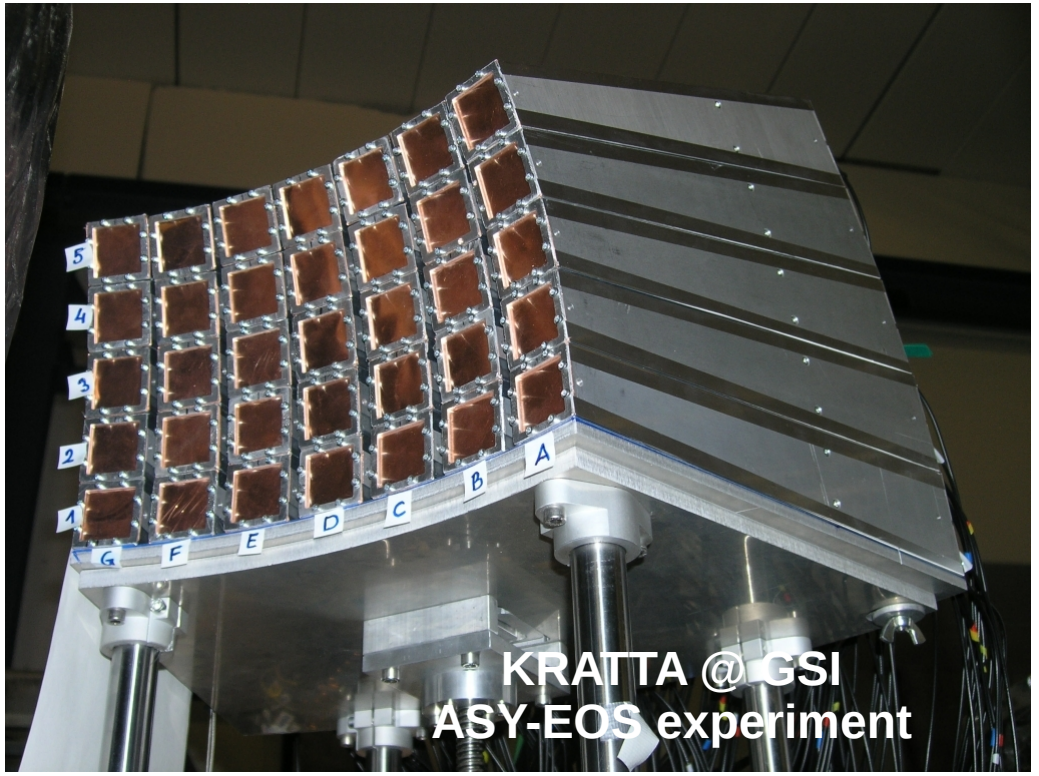

KRATTA main characteristics

- Broad energy range (from ~2.5 to ~260 MeV for protons)
- Mass resolution up to Z~4
- Modularity, versatility, portability (35 modules)
- Solid angle ~160 msr (~4.5 msr/module at 40 cm from the target)
- Low noise preamplifiers
- Digital pulse processing (15×V1724 CAEN FADCs (100 MHz, 14 bits)
- Off-line pulse shape analysis
- VME+RIO4+MBS data acquisition
- Operates in air (at present)

Angles

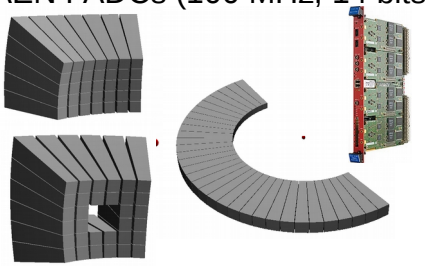

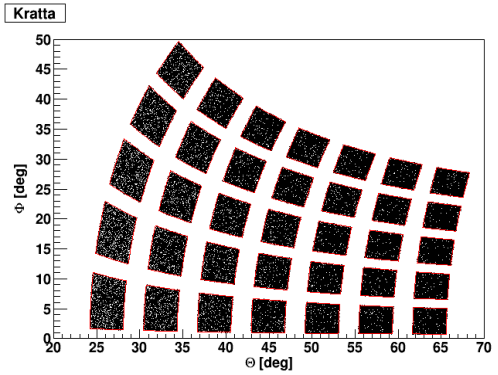

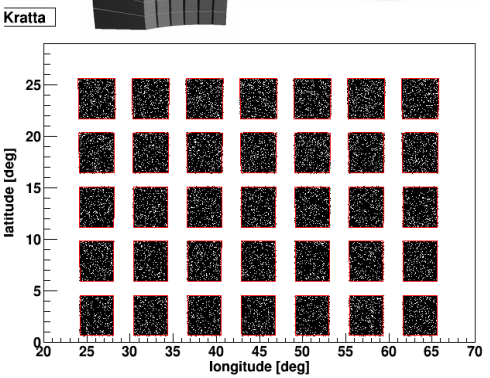

Thresholds

Fragment	E_{low} (500 μm Si) [MeV/u]	E_{int} (2.5 cm CsI) [MeV/u]	E_{up} (15 cm CsI) [MeV/u]
^{1}H	8.3	89.6	254.4
^{4}He	8.3	89.4	253.9
^{7}Li	9.5	103.6	296.5
^{20}Ne	19.9	231.3	719.0
^{43}Ca	26.7	339.7	1134.2
^{91}Zr	34.0	513.9	1911.8
^{197}Au	38.6	775.8	3550.9

KRATTA active elements

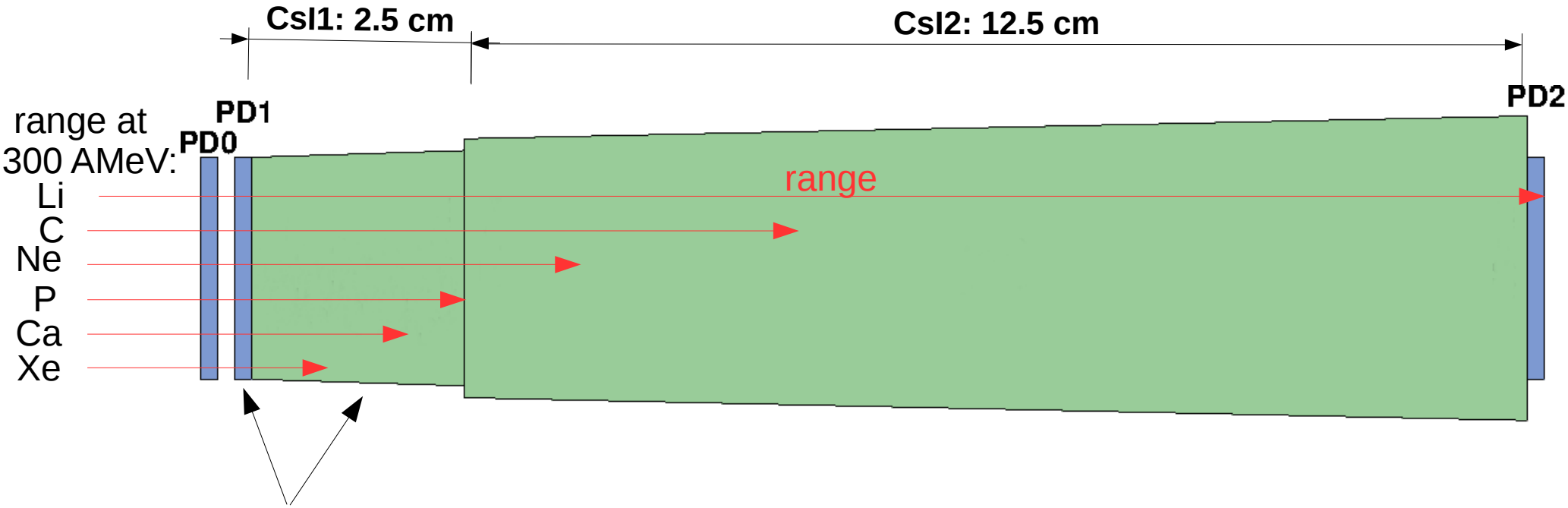

PD1+CSI1=SCT (Single Chip Telescope, G. Pasquali et al. NIMA 301(91)101)

Photodiodes: HAMAMATSU S5377-02

- Active Area: 28x28 mm^2
- Thickness: 500 ± 15 μm
- Orientation: (111)
- Dead Layers: 1.5 μm front, 20 μm rear
- Full Depletion: ~170 V
- Dark Current: 30 nA, (Max. 150 nA)
- Rise Time: 40 ns
- Capacitance: 200 pF

CsI(Tl): IMP-CAS, Lanzhou, China

- Tl concentration: 1500 ppm
- LO non-uniformity: <7%
- Shape: Truncated pyramids
- Tolerance: ± 0.1 mm

Wrapping: 3M Vikuiti™ ESR foil

- Reflectance: >98%
- Thickness: 65 μm

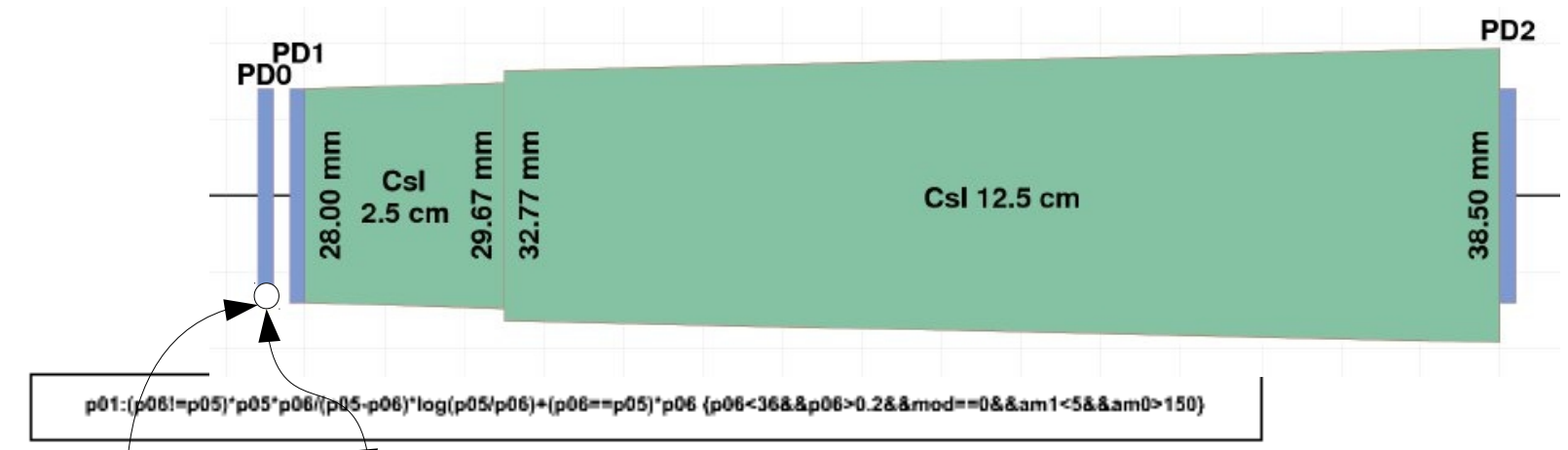

p01:(p06!=p05)*p05*p06/(p05-p06)*log(p05/p06)+(p06==p05)*p06 {p06<36&&p06>0.2&&mod==0&&am1<5&&am0>150}

ID map for particles **stopped** in **PD0**
after pulse shape analysis

Identification threshold
reduced by a factor of ~3

^{6,7,8}Li

^{3,4,6}He

p,d,t

Amplitude PD0

Mode of current signal PD0

SCT decomposed (non-trivial)

(lines from the ATIMA range-energy tables)

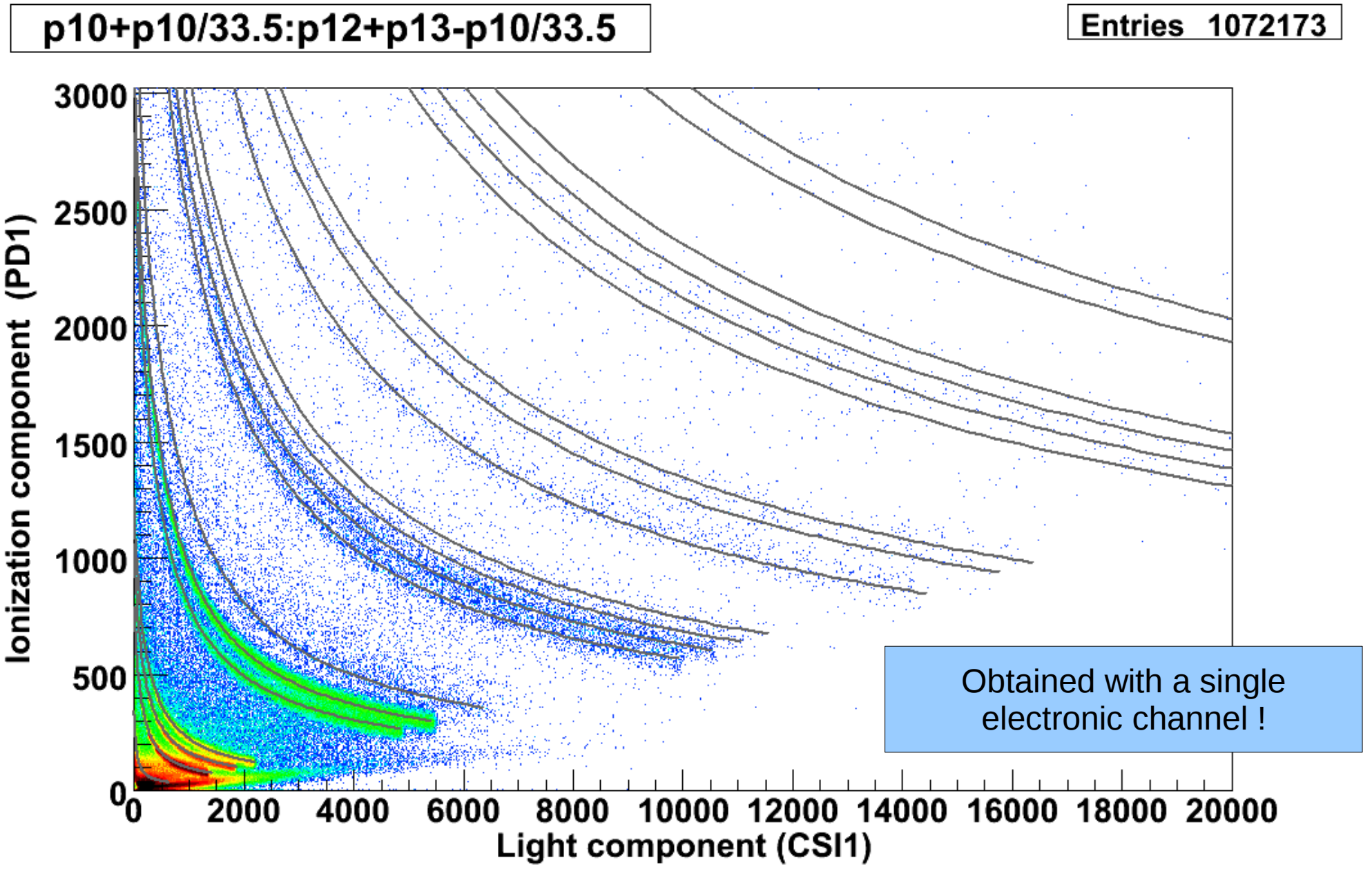

KRATTA@HIMAC: ΔE-E

Xe fragmentation at ~300 AMeV

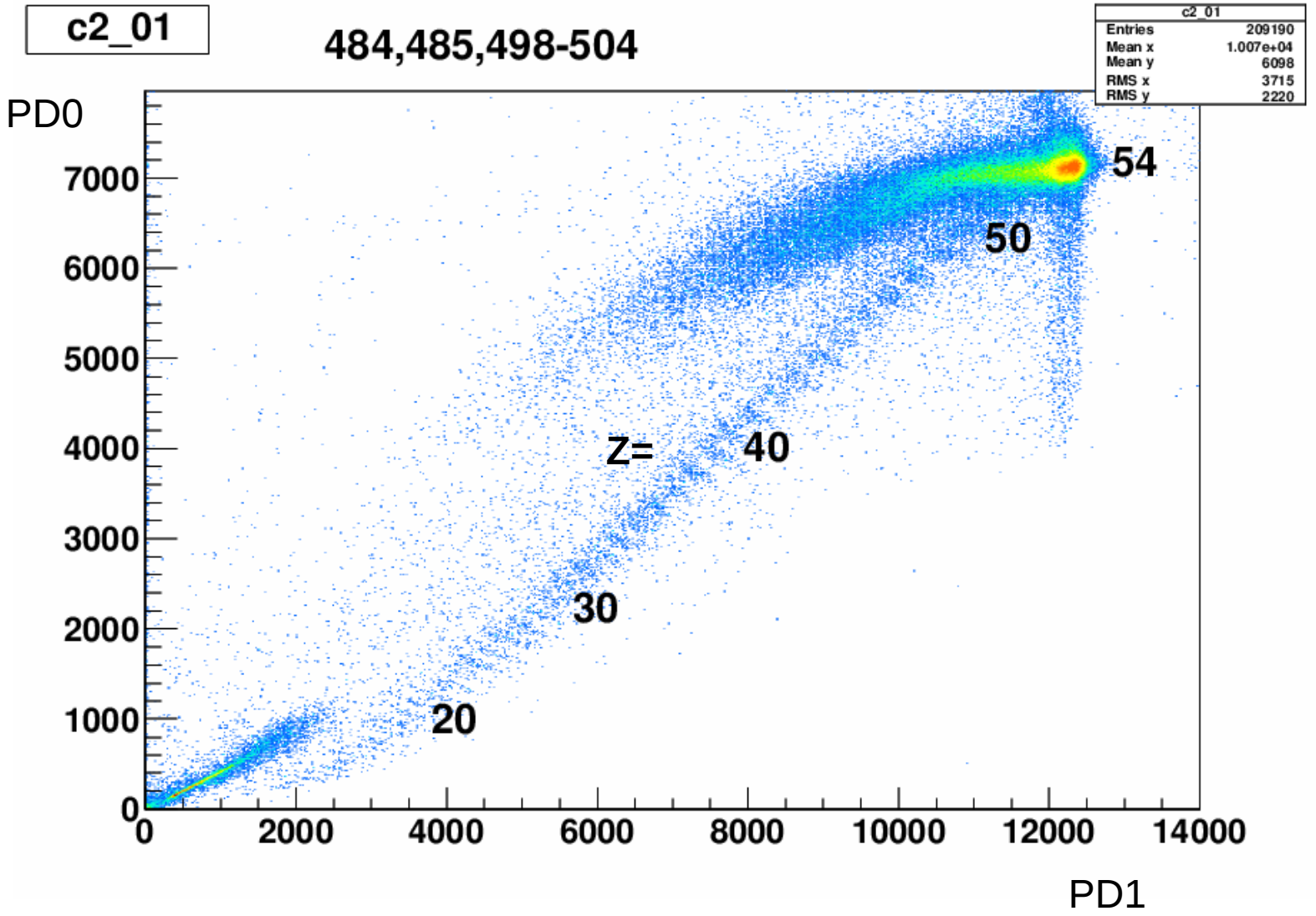

Low gain settings

Flows of light charged particles in Au (400 MeV/u) + Au reactions: KRATTA vs FOPI results

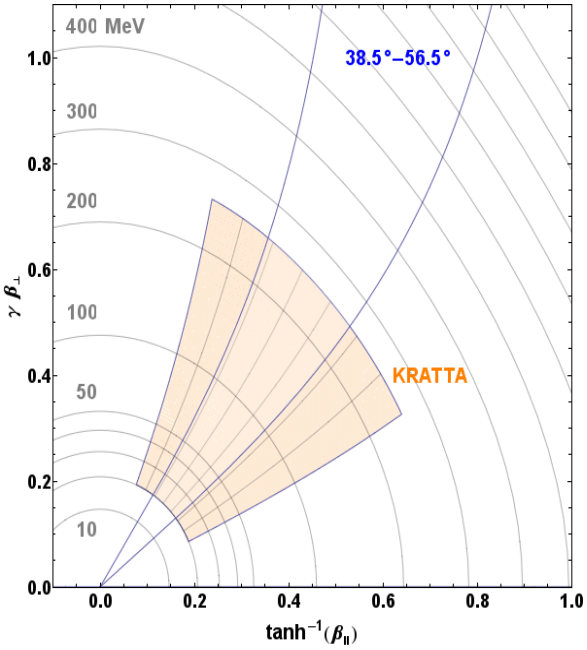

Fourier decomposition of the azimuthal distributions with respect to the reaction plane (ϕ_R) :

$$\frac{dN}{d(\phi-\phi_R)} = \frac{N_0}{2\pi}\left(1+2\sum_{n\geq 1} v_n \cos n(\phi-\phi_R)\right)$$

$v_1 \equiv \langle \cos(\phi-\phi_R)\rangle$ directed flow

$v_2 \equiv \langle \cos 2(\phi-\phi_R)\rangle$ elliptic flow

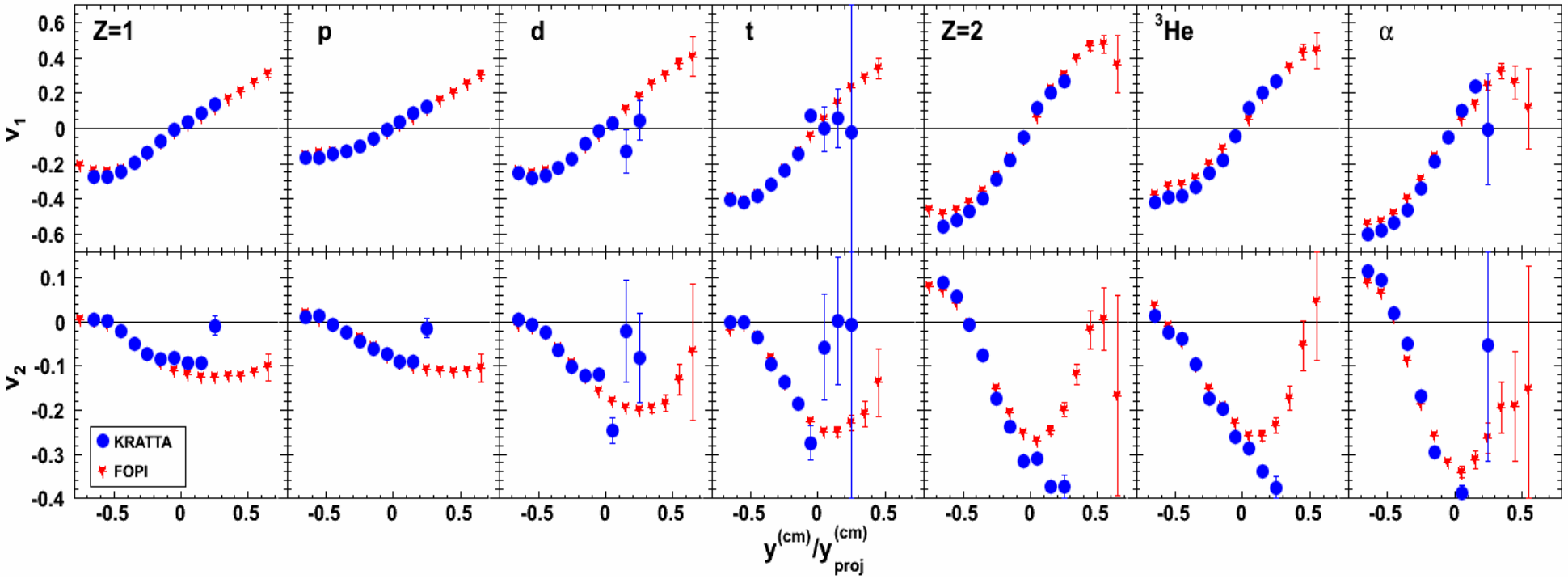

Model simulations

UrQMD Q. Li, J.Phys. G 31(2005)1359

„Fermi-gas" parametrization of the symmetry term:

$$E_{sym} = E_{sym}^{pot} + E_{sym}^{kin} = 22\ \text{MeV}\left(\frac{\rho}{\rho_o}\right)^{\gamma} + 12\ \text{MeV}\left(\frac{\rho}{\rho_o}\right)^{2/3}$$

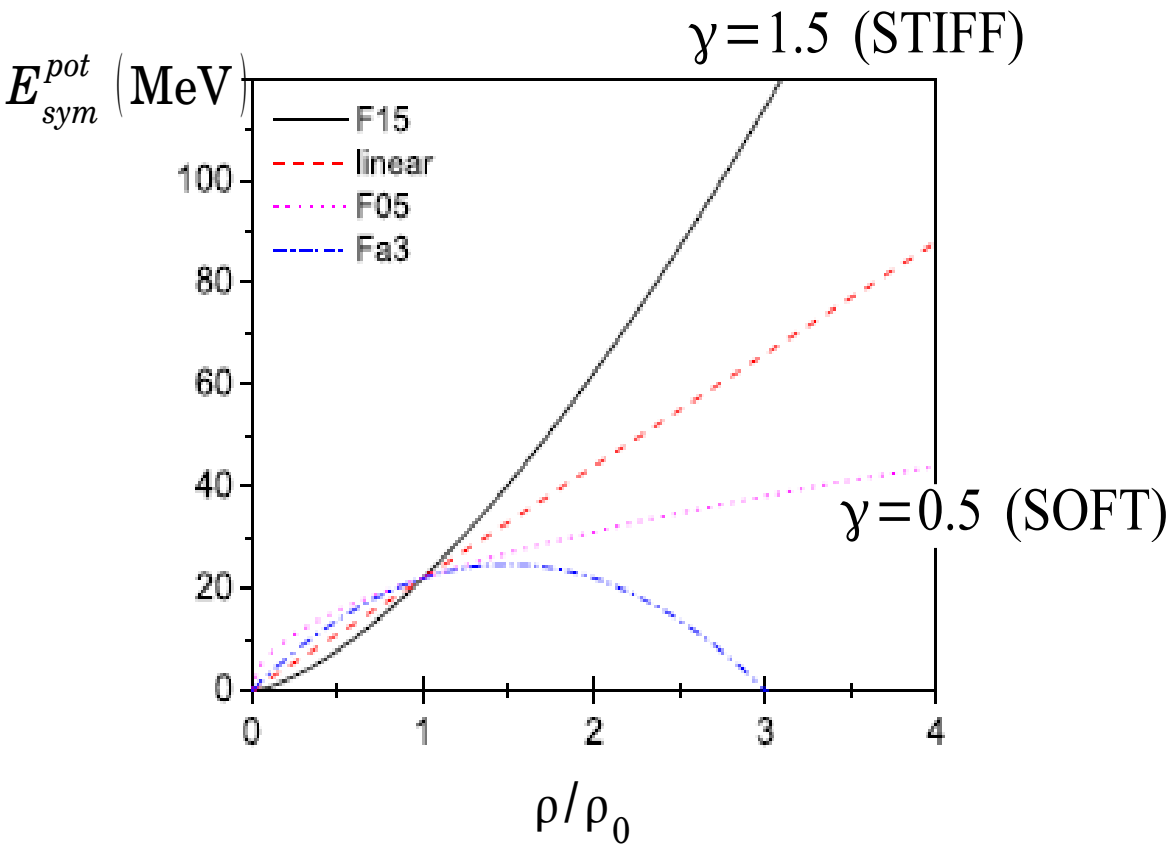

Stopping time = 150 fm/c

Nucleons → $\{\vec{r}_i, \vec{p}_i\}$

Clustering procedure

($\Delta r = 2.5$ fm, $\Delta p = 290$ MeV/c)

($\Delta r = 3$ fm, $\Delta p = 100$ MeV/c)

⋮

Charge distribution Au (400 MeV/u) + Au

KRATTA data ⟷ **UrQMD predictions**

ASY - SOFT

ASY - STIFF

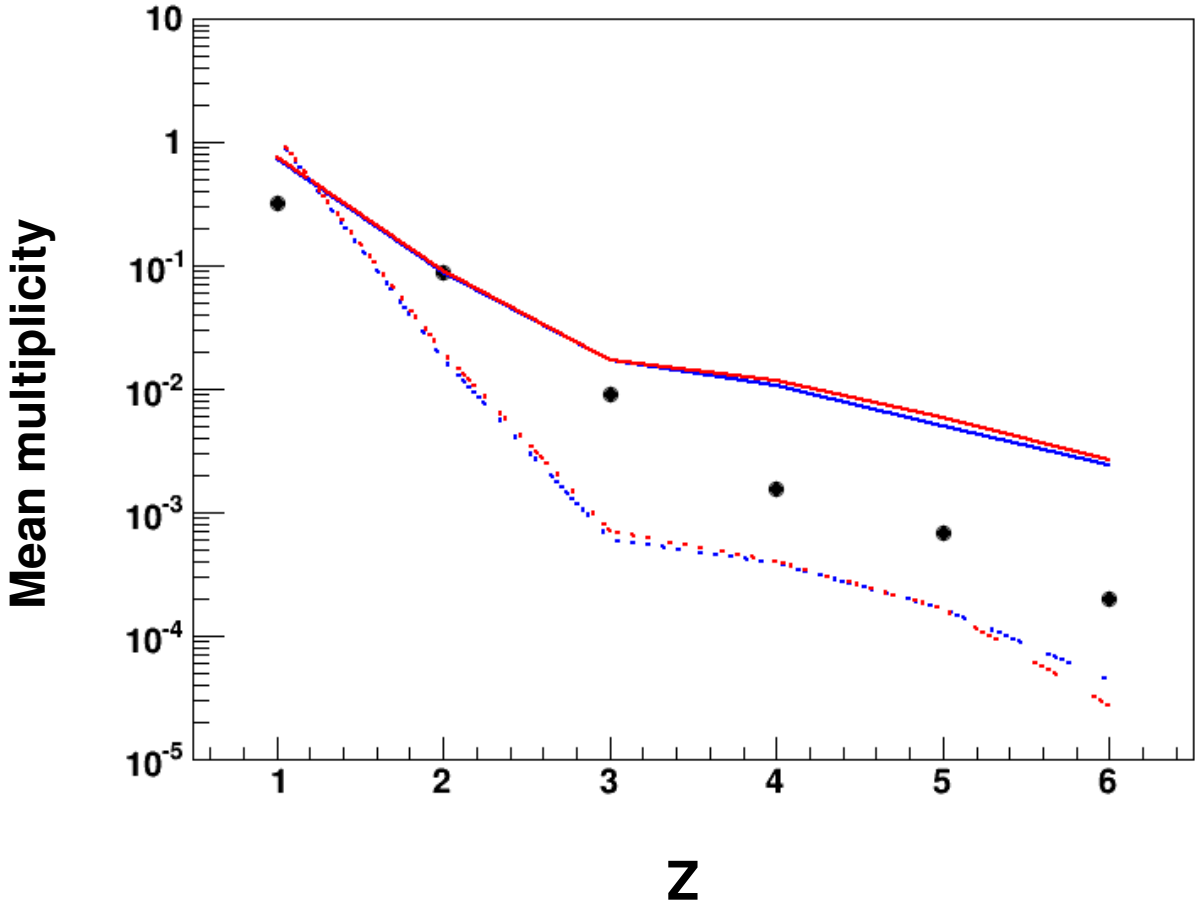

b < 7.5 fm

24° < lon < 59.4°

0.7° < lat < 25.7°

20 < E_{KIN}/A < 133 MeV

Δr=2.5fm Δp=290MeV/c γ=0.5

Δr=2.5fm Δp=290MeV/c γ=1.5

Δr=3.0fm Δp=100MeV/c γ=0.5

Δr=3.0fm Δp=100MeV/c γ=1.5

Exp.

Energy/nucleon

Au (400 MeV/u) + Au

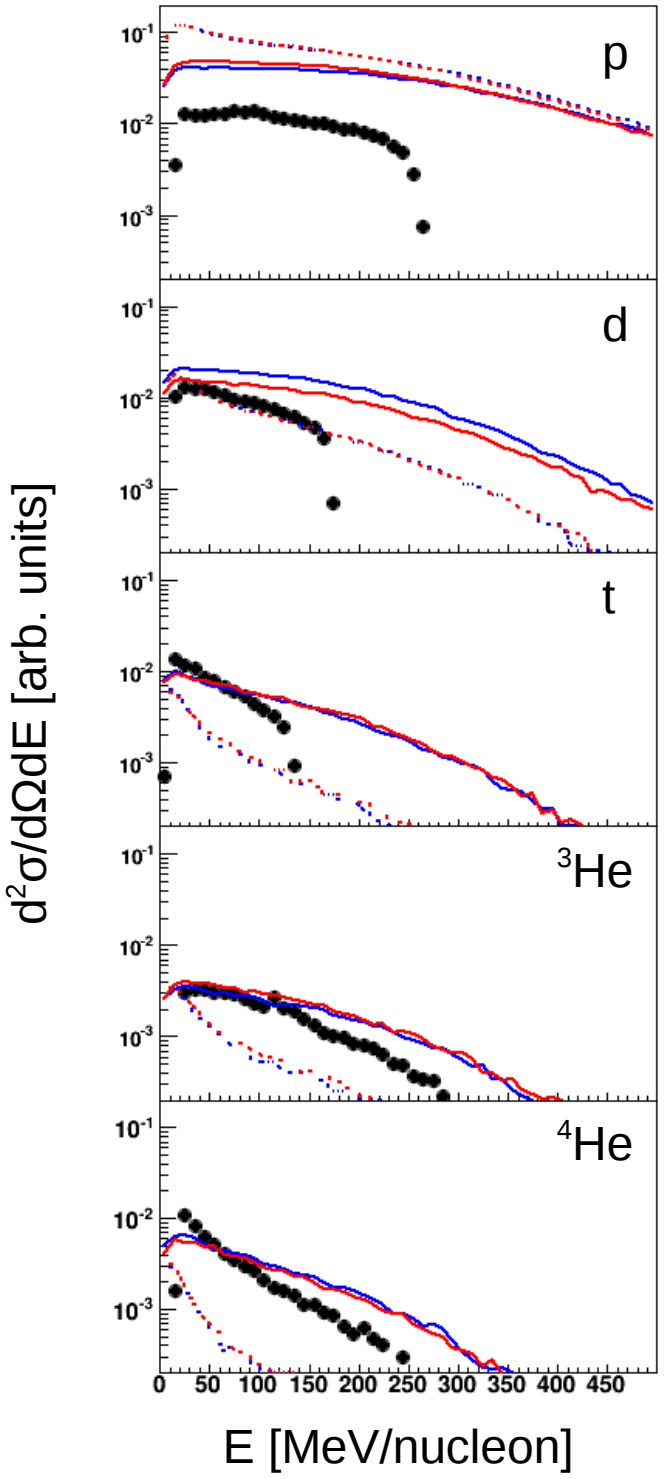

Δr=2.5fm Δp=290MeV/c γ=0.5

Δr=2.5fm Δp=290MeV/c γ=1.5

Δr=3.0fm Δp=100MeV/c γ=0.5

Δr=3.0fm Δp=100MeV/c γ=1.5

Exp.

b < 7.5 fm

24° < lon < 59.4°

0.7° < lat < 25.7°

t/^{3}He isotope ratios ($20 < E_{kin}/A < 133$ MeV)

Au(400 MeV/u) + Au

5.5 < b < 7.5 fm

24° < Θ_{LAB} < 62°

20 < E_{KIN}/A < 133 MeV

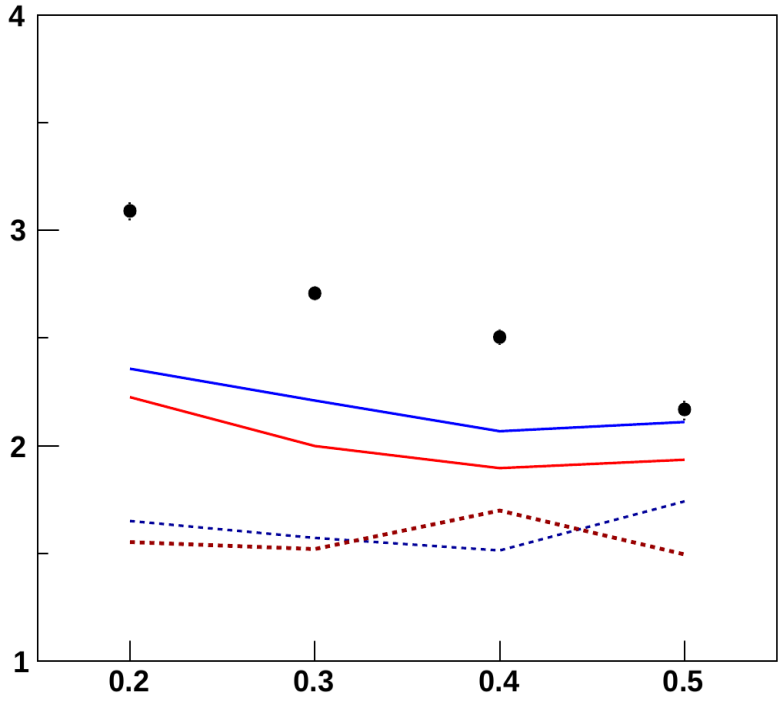

y / y_{proj}

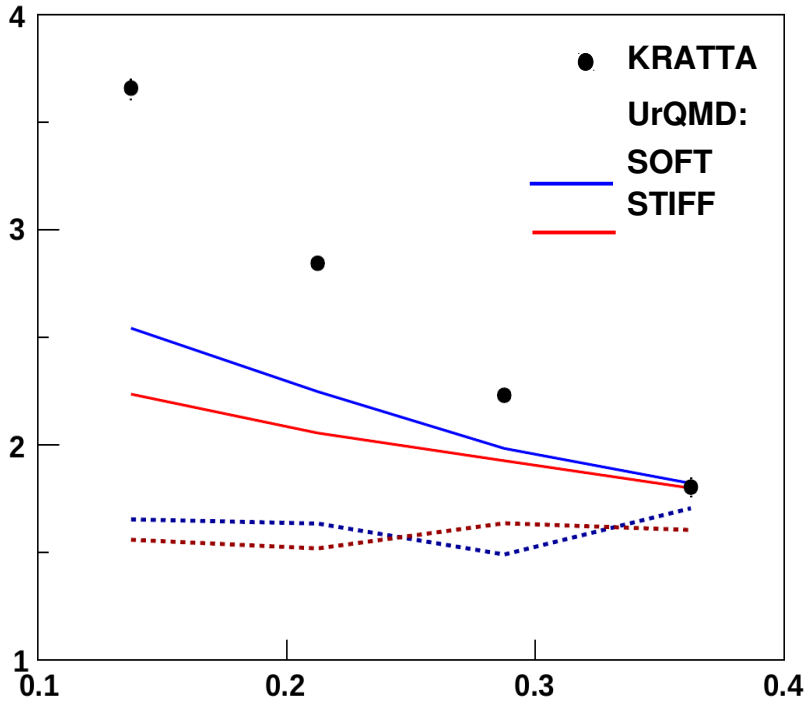

p_T/A (GeV/c)

Proton flow ($20 < E_{kin} < 250$ MeV)

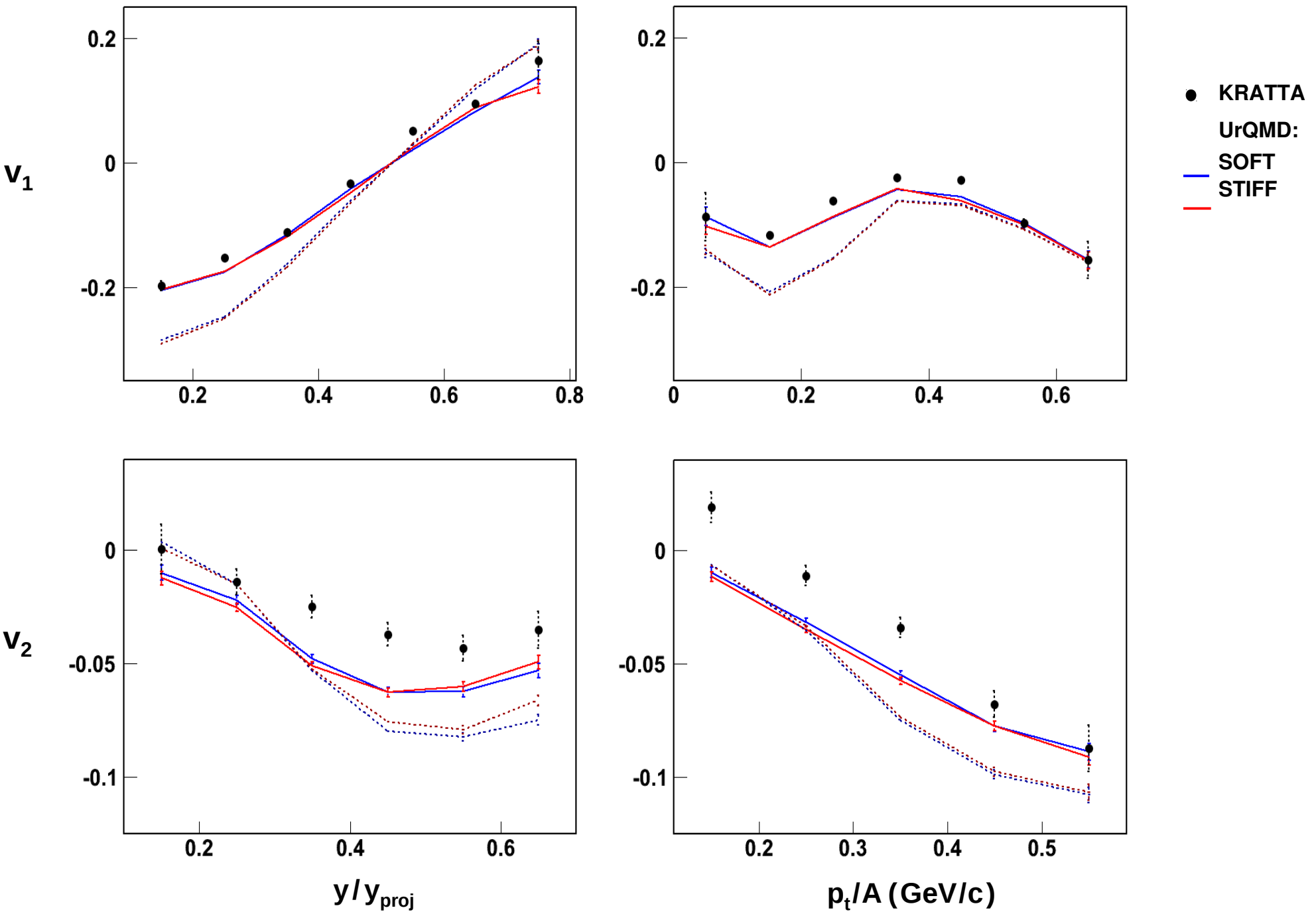

Deuteron flow ($20 < E_{kin}/A < 160$ MeV)

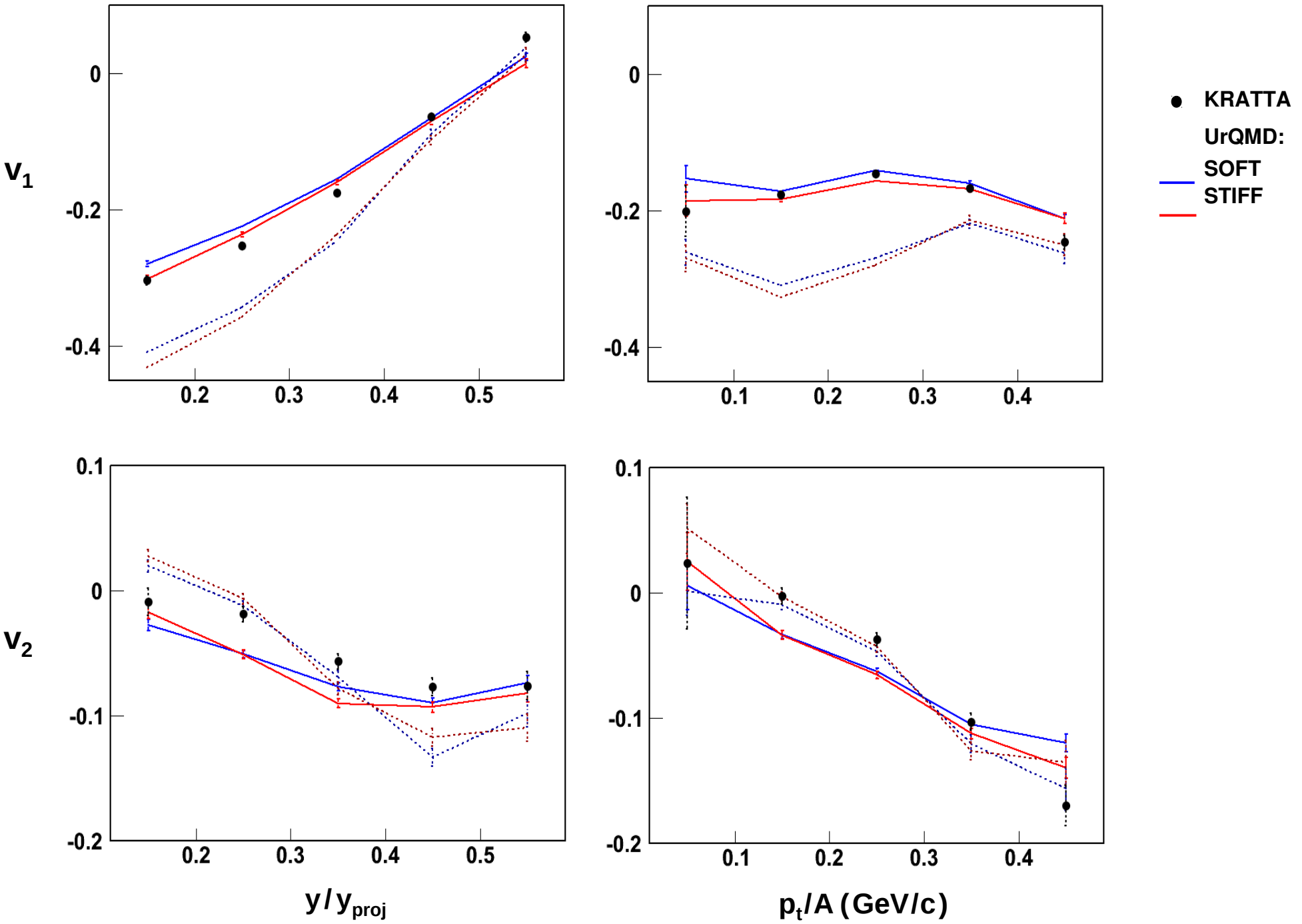

CHIMERA@ASY-EOS

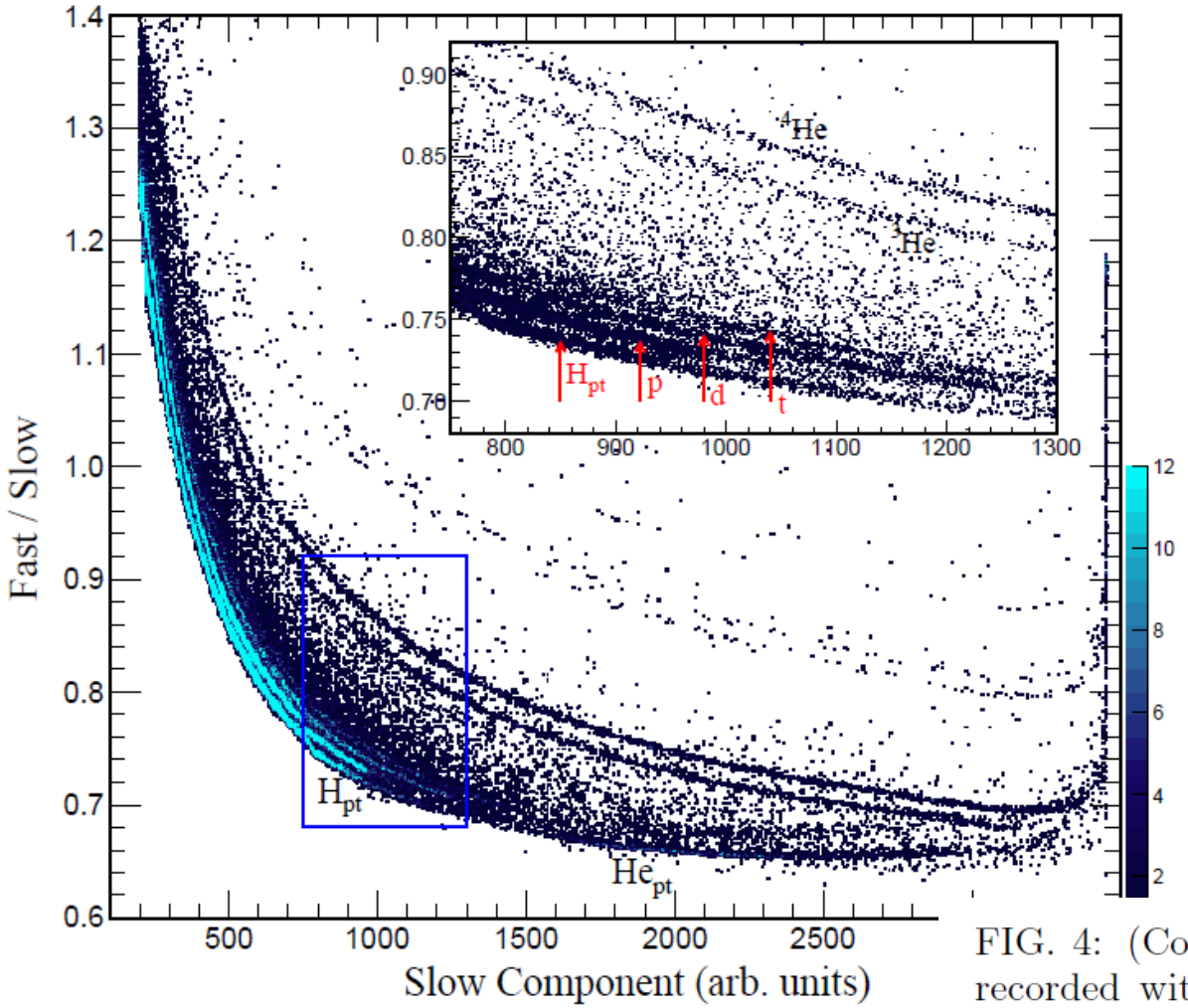

FIG. 4: (Color online) Identification plot of CsI(Tl) signals recorded with a CHIMERA module of ring 7 ($\theta_{\rm lab} \approx 17°$) from ^{197}Au+^{197}Au collisions at 400 MeV/nucleon displaying the ratio of fast-over-slow vs. the slow signal components. The loci of hydrogen and helium ions punching through the full length of the detector are labeled as H_{pt} and He_{pt}. An expanded view of the area within the rectangular box is shown in the inset. Besides the punch-through groups, also the loci of mass-identified light ions are indicated there.

P. Russotto et al., to be published

ALADIN ToF Wall@ASY-EOS

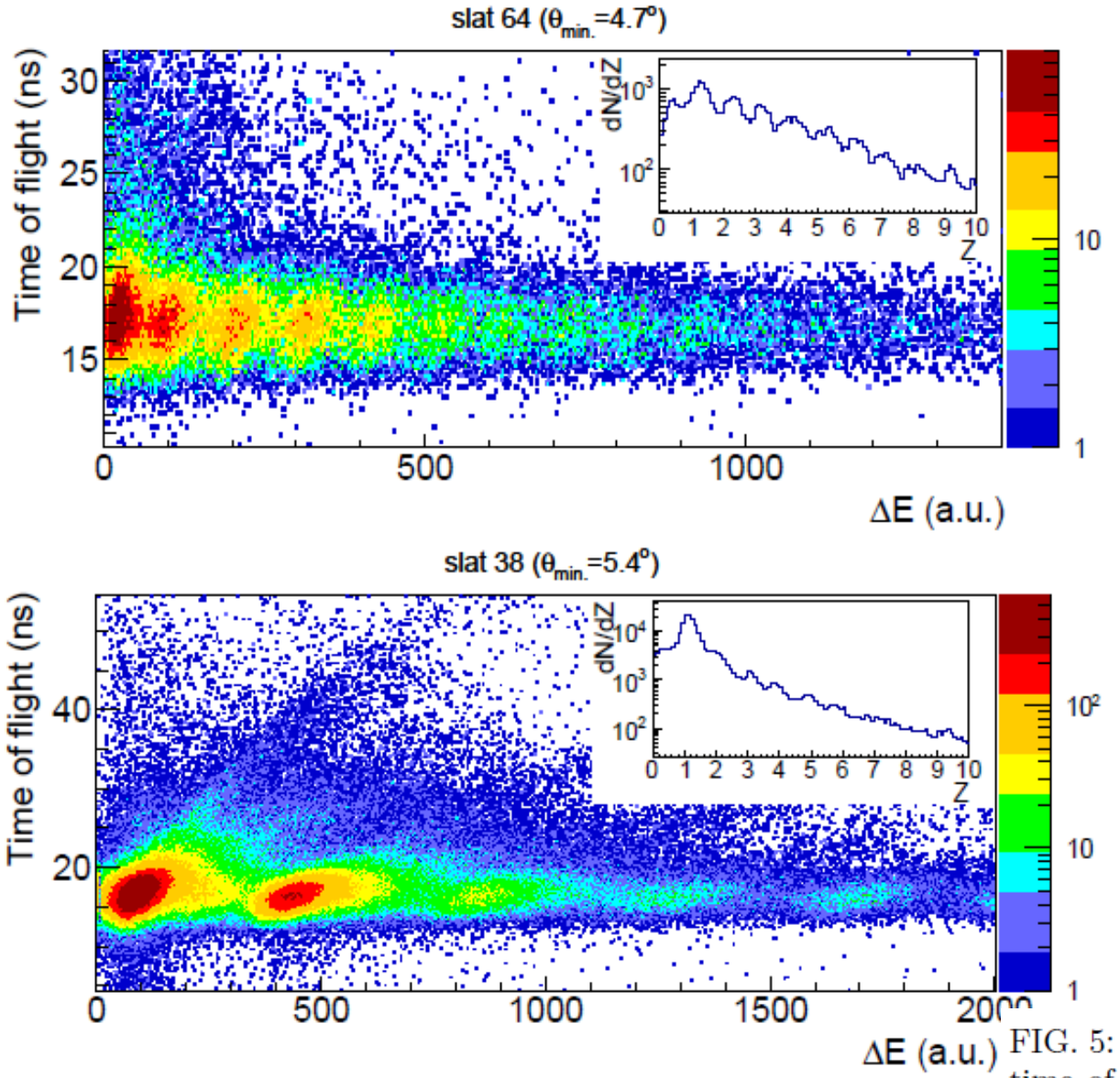

FIG. 5: (Color online) AToF identification plots of calibrated time of flight vs. recorded energy loss ΔE for two slats approximately 30 cm and 35 cm to the right of the beam direction ($\theta_{\rm lab} \approx 4.7^\circ$ and $\approx 5.4^\circ$, respectively, at their central parts). The groups of light elements are clearly recognized up to atomic number $Z \approx 10$ as shown in the inset.

P. Russotto et al., to be published

FOPI-LAND

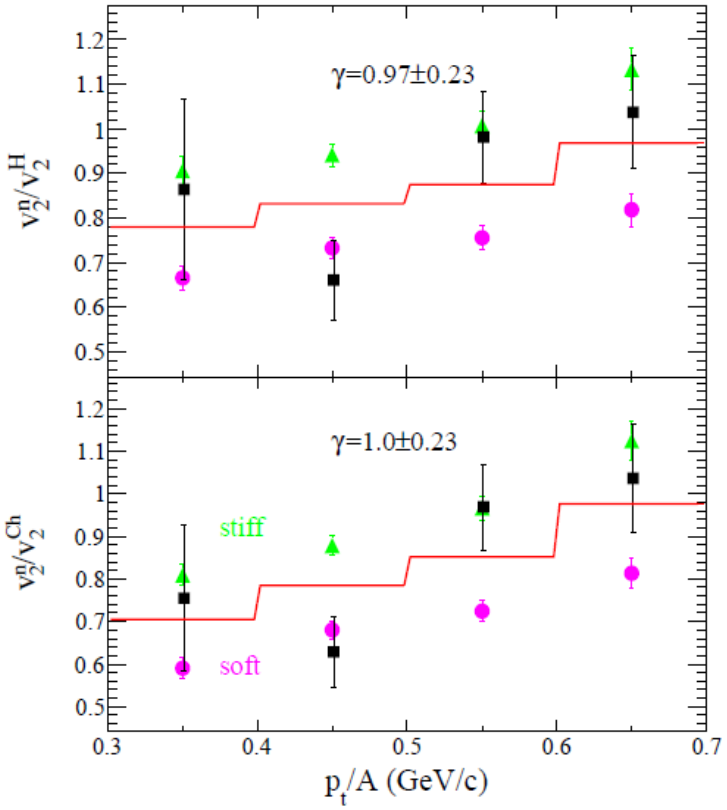

FIG. 14: (Color online) FOPI-LAND data: Elliptic flow ratio of neutrons over all hydrogen isotopes (top) and of neutrons over all charged particles (bottom) for moderately central ($b <$ 7.5 fm) collisions of ^{197}Au+^{197}Au at 400 MeV/nucleon, as a function of the transverse momentum per nucleon p_t/A. The black symbols represent the experimental data. The UrQMD predictions for stiff ($\gamma = 1.5$, green symbols) and soft ($\gamma = 0.5$, purple symbols) are shown. The red line in each panel is the result of a linear interpolation between the predictions; the obtained gamma values and their uncertainties are indicated.

LAND@ASY-EOS

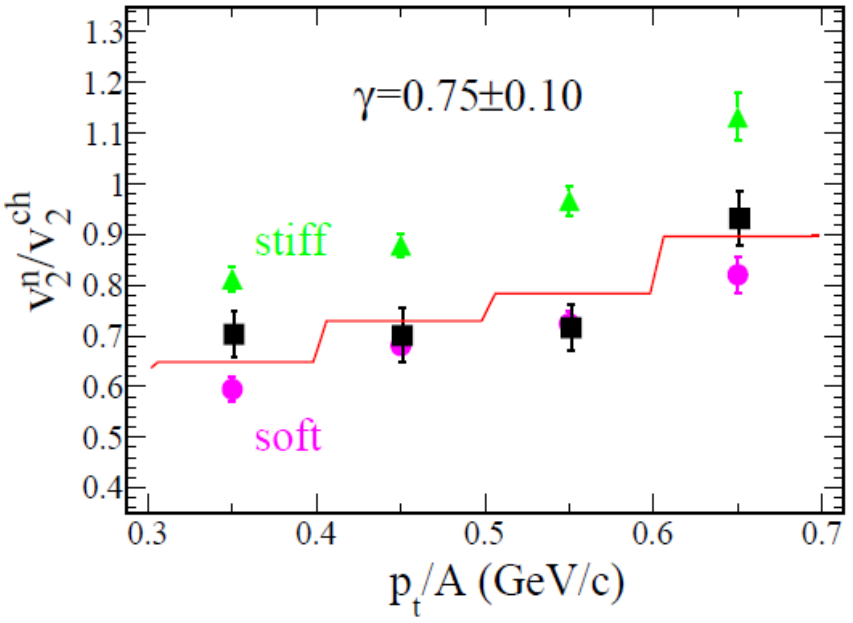

FIG. 15: (Color online) Elliptic flow ratio of neutrons and charged particles for moderately central ($b <$ 7.5 fm) collisions of ^{197}Au+^{197}Au at 400 MeV/nucleon as a function of the transverse momentum per nucleon p_t/A, evaluated with a fraction of 80% for the second step of timing corrections (see Sec. IV A). The full squares represent the experimental data, the triangles and dots represent the UrQMD predictions for stiff ($\gamma = 1.5$) and soft ($\gamma = 0.5$) power-law exponents of the potential term. The full line is the result of a linear interpolation between the predictions, leading to the indicated $\gamma = 0.75 \pm 0.10$.

P. Russotto et al., to be published

LAND@ASY-EOS

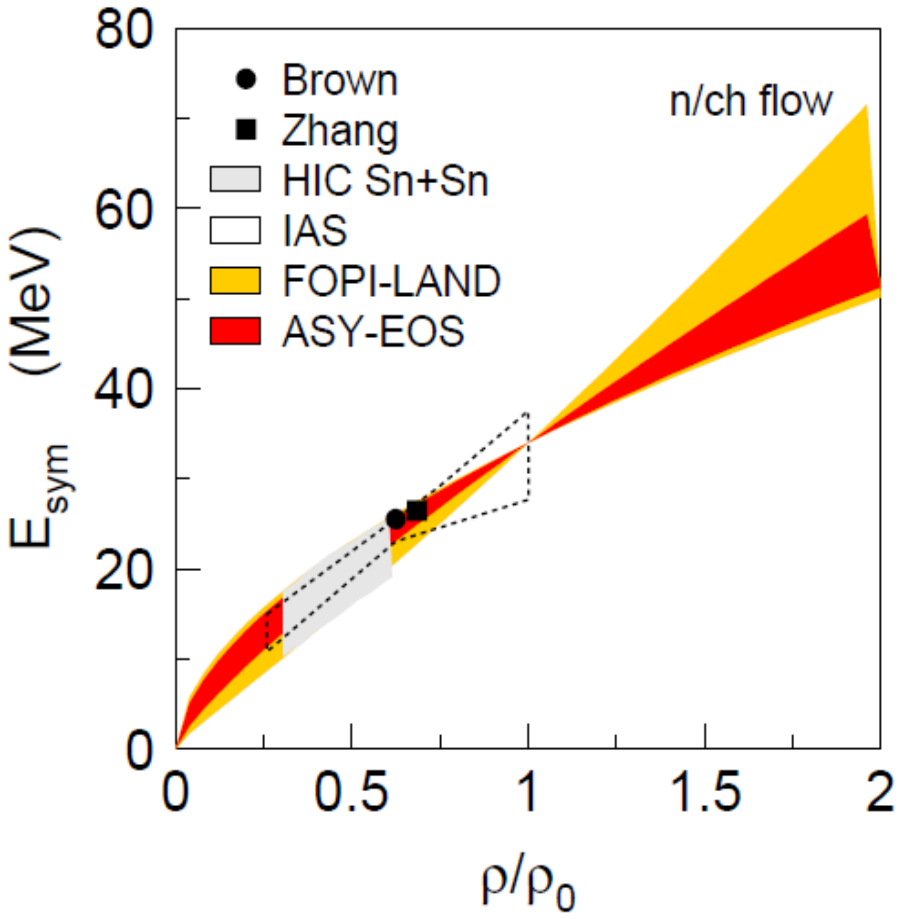

$\gamma = 0.72 \pm 0.19$

$L = 72 \pm 13$ MeV

P. Russotto et al., to be published

FIG. 19: (Color online) Constraints deduced for the density dependence of the symmetry energy from the present data in comparison with the FOPI-LAND result of Ref. [5] as a function of the reduced density ρ/ρ_0. For reference, the low-density results of Refs. [66–69] as presented in Ref. [70] are included.

Conclusions

KRATTA

- **good detector performance**
- **usefulness of photodiodes operating in the double mode**

KRATTA results from the ASY-EOS measurements

- **flow parameters consistent with FOPI data**
- **UrQMD (+ clustering) fails in reproducing isotope ratios**
- **realistic description of cluster formation needed**

LAND results from the ASY-EOS measurements

- **moderately soft to linear density dependence: $\gamma = 0.72 \pm 0.19$**

The ASY-EOS Collaboration

P. Russotto,[1] S. Gannon,[2] S. Kupny,[3] P. Lasko,[3] L. Acosta,[4] M. Adamczyk,[3] A. Al-Ajlan,[5] M. Al-Garawi,[6] S. Al-Homaidhi,[5] F. Amorini,[4] L. Auditore,[7,8] T. Aumann,[9] Y. Ayyad,[10] V. Baran,[4,11] Z. Basrak,[12] R. Bassini,[13] J. Benlliure,[10] C. Boiano,[13] M. Boisjoli,[14] K. Boretzky,[15] J. Brzychczyk,[3] A. Budzanowski,[16,*] C. Caesar,[9] G. Cardella,[1] P. Cammarata,[17] Z. Chajecki,[18] M. Chartier,[2] A. Chbihi,[14] M. Colonna,[4] M. D. Cozma,[19] B. Czech,[16] E. De Filippo,[1] M. Di Toro,[4,20] M. Famiano,[21] I. Gašparić,[9,12] V. Greco,[4,20] L. Grassi,[12] C. Guazzoni,[13,22] P. Guazzoni,[13,23] M. Heil,[15] L. Heilborn,[17] R. Introzzi,[24] T. Isobe,[25] K. Kezzar,[6] M. Kiš,[12,15] A. Krasznahorkay,[26] N. Kurz,[15] E. La Guidara,[1] G. Lanzalone,[4,27] A. Le Fèvre,[15] Y. Leifels,[15] R. C. Lemmon,[28] Q. F. Li,[29] I. Lombardo,[30,31] J. Łukasik,[16] W. G. Lynch,[18] P. Marini,[14,32] Z. Matthews,[2] L. May,[17] T. Minniti,[1] M. Mostazo,[10] A. Pagano,[1] M. Papa,[1] P. Pawłowski,[16] S. Pirrone,[1] G. Politi,[1,20] F. Porto,[4,20] W. Reisdorf,[15] W. Reviol,[33] F. Riccio,[13,22] F. Rizzo,[4,20] E. Rosato,[30,31,*] D. Rossi,[15,18] S. Santoro,[7,8] D. G. Sarantites,[33] H. Simon,[15] I. Skwirczynska,[16] Z. Sosin,[3,*] L. Stuhl,[26] W. Trautmann,[15] A. Trifirò,[7,8] M. Trimarchi,[7,8] M. B. Tsang,[18] G. Verde,[1] M. Veselsky,[34] M. Vigilante,[30,31] Yongjia Wang,[29] A. Wieloch,[3] P. Wigg,[2] J. Winkelbauer,[18] H. H. Wolter,[35] P. Wu,[2] S. Yennello,[17] P. Zambon,[13,22] L. Zetta,[13,23] and M. Zoric[12]

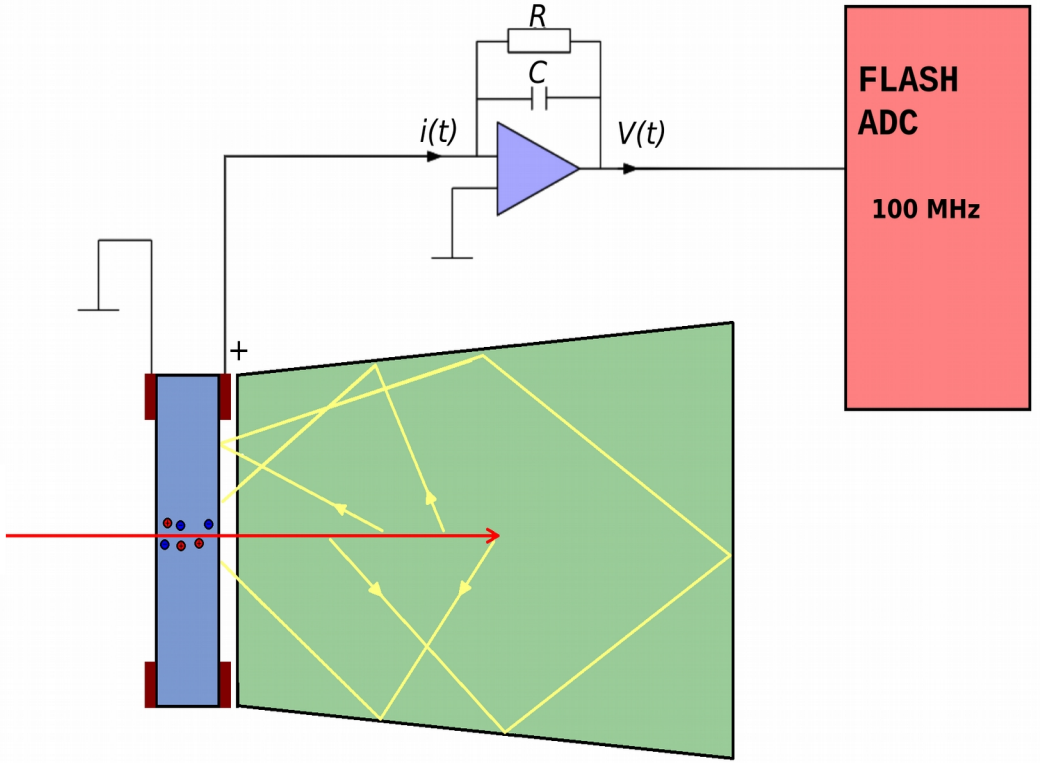

Silicon PIN photodiode

CsI(Tl) scintillator

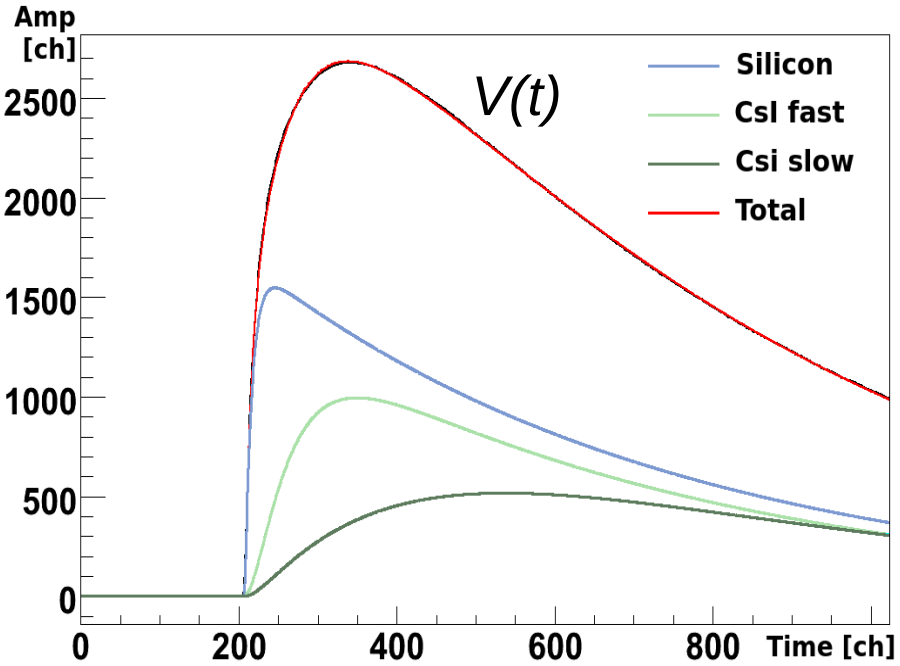

Pulse decomposition analysis

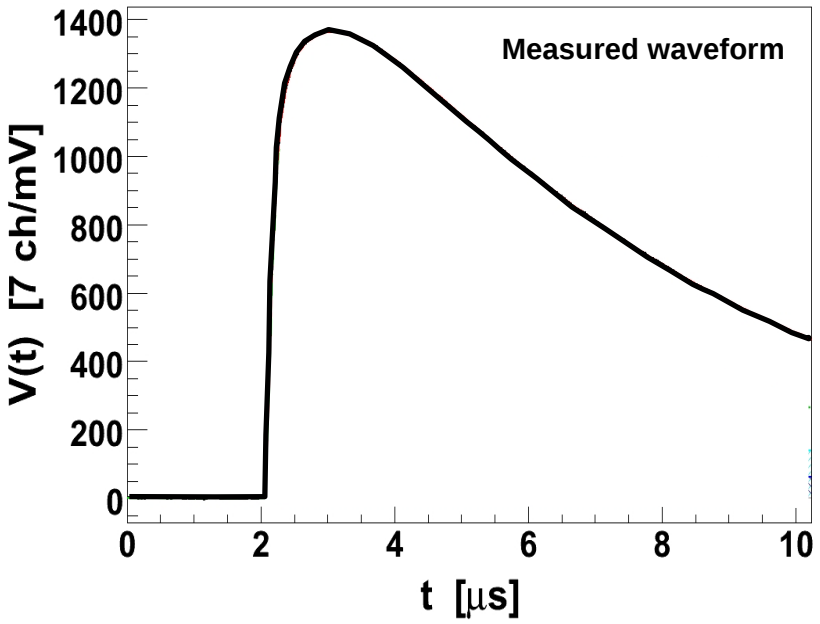

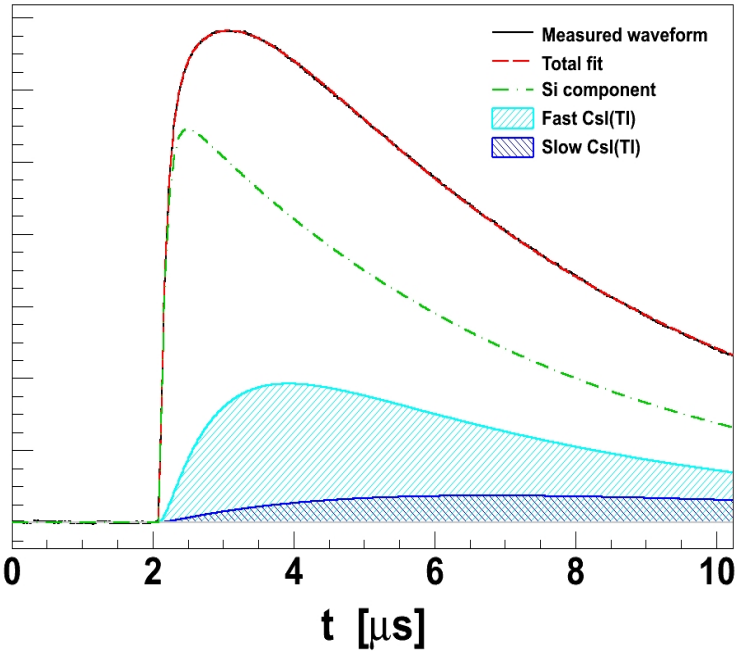

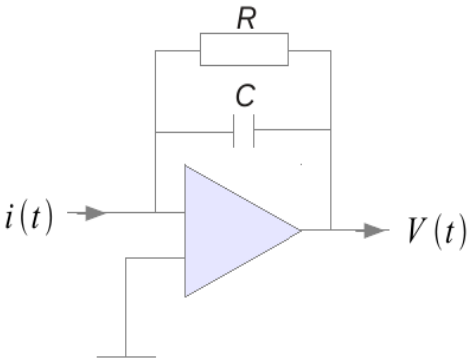

$$\frac{dV(t)}{dt}+\frac{1}{RC}V(t)=\frac{i(t)}{C}$$

$$\frac{Q_1\left(e^{-t/\tau_1}-e^{-t/\tau_2}\right)}{\tau_1-\tau_2}=i(t) \Rightarrow V(t)=Q_1RC\left(\frac{e^{-t/RC}RC}{(RC-\tau_1)(RC-\tau_2)}+\frac{e^{-t/\tau_1}\tau_1}{(\tau_1-RC)(\tau_1-\tau_2)}+\frac{e^{-t/\tau_2}\tau_2}{(\tau_2-\tau_1)(\tau_2-RC)}\right)$$

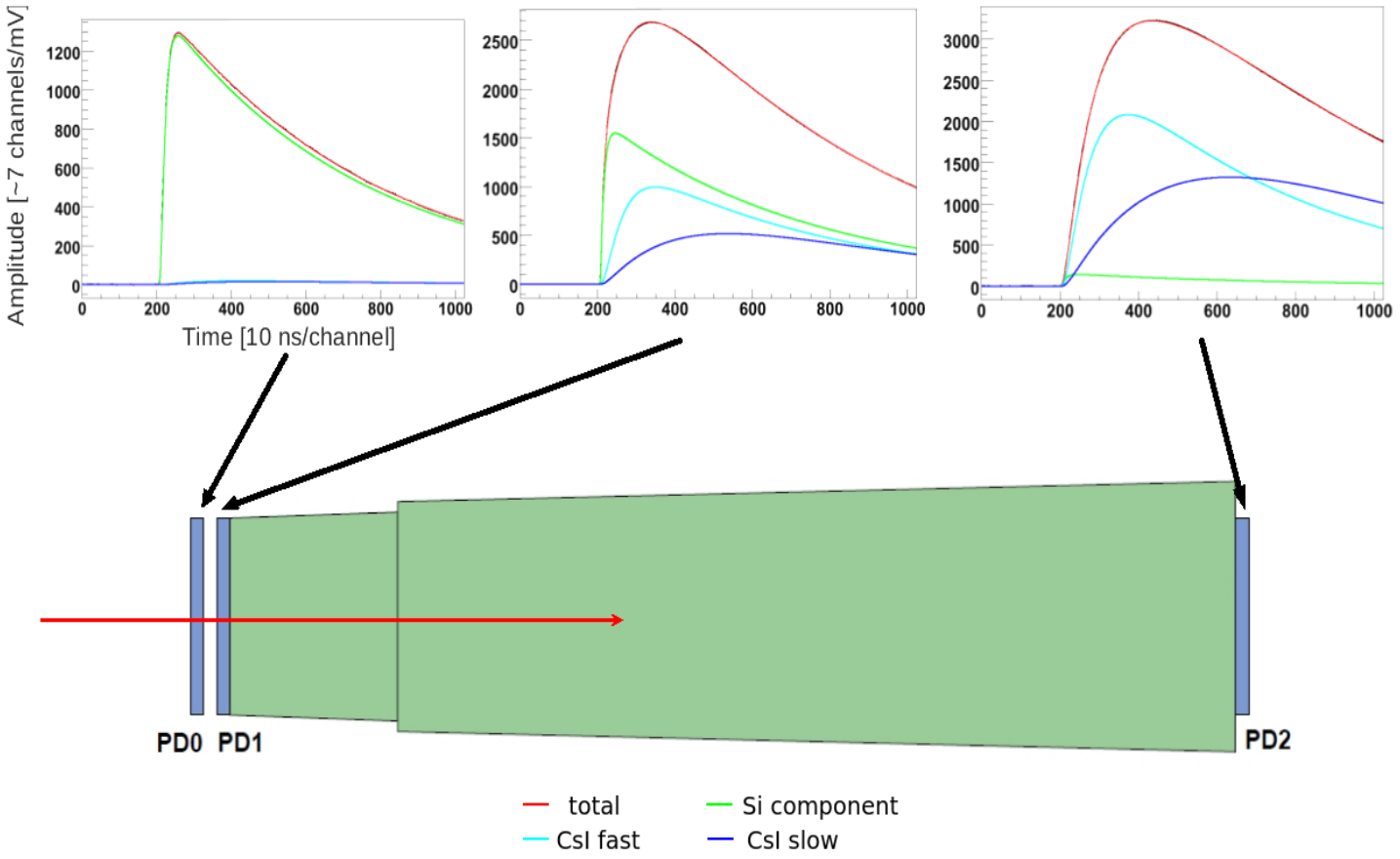
Amplitude [~7 channels/mV]
Time [10 ns/channel]
PD0
PD1
PD2
total
Si component
CsI fast
CsI slow

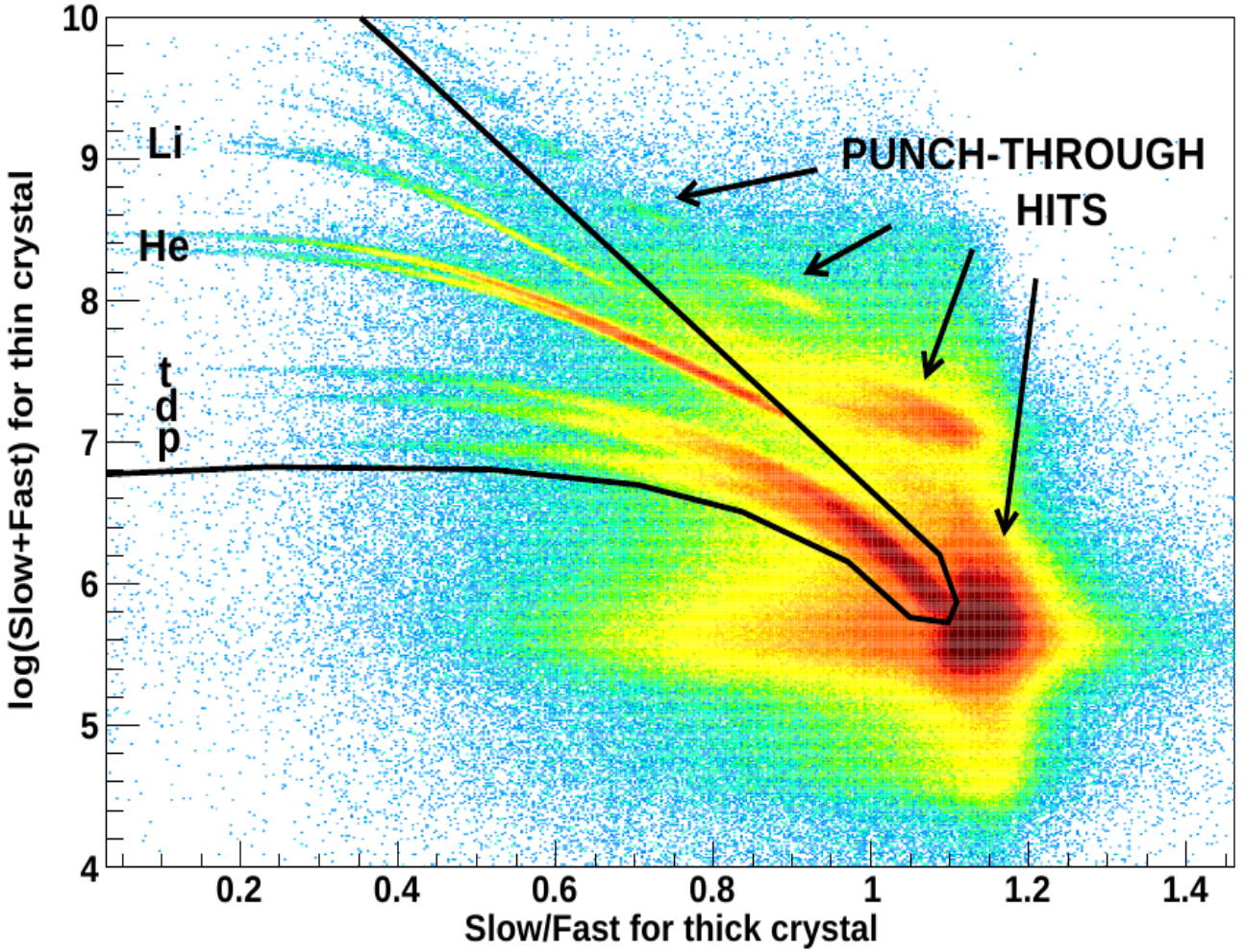
log(Slow+Fast) for thin crystal
Slow/Fast for thick crystal
10
9
8
7
6
5
4
0.2
0.4
0.6
0.8
1
1.2
1.4
Li
He
t
d
p
PUNCH-THROUGH
HITS